ISSN: 0256-307X

中国物理快报

Chinese Physics Letters

Volume 34 Number 10 October 2017

A Series Journal of the Chinese Physical Society
Distributed by IOP Publishing

Online: http://iopscience.iop.org/0256-307X
http://cpl.iphy.ac.cn

CHINESE PHYSICAL SOCIETY
IOP Publishing

CHIN. PHYS. LETT. Vol. 34, No. 10 (2017) 104204

Imaging Transparent Objects in a Turbid Medium Using a Femtosecond Optical Kerr Gate *

Yi-Peng Zheng(郑益朋)[1], Jin-Hai Si(司金海)[1**], Wen-Jiang Tan(谭文疆)[1], Xiao-Jing Liu(刘晓晶)[1], Jun-Yi Tong(佟俊仪)[2], Xun Hou(侯洵)[1]

[1]*Key Laboratory for Physical Electronics and Devices of the Ministry of Education of China, and Shaanxi Key Lab of Information Photonic Technique, School of Electronics and Information Engineering, Xi'an Jiaotong University, Xi'an 710049*

[2]*Departments of Applied Physics, Xi'an University of Technology, Xi'an 710049*

(Received 29 June 2017)

A femtosecond optical Kerr gate time-gated ballistic imaging method is demonstrated to image a transparent object in a turbid medium. The shape features of the object are obtained by time-resolved selection of the ballistic photons with different optical path lengths, the thickness distribution of the object is mapped, and the maximum is less than 3.6%. This time-resolved ballistic imaging has potential applications in studying properties of the liquid core in the near field of the fuel spray.

PACS: 42.65.Pc, 42.25.Fx, 42.65.Hw DOI: 10.1088/0256-307X/34/10/104204

The imaging of objects in scattering media has always been a topic of intense research for industrial, medical, and military applications. Numerous significant studies on transillumination imaging through scattering media have been reported recently.[1–9] When a light beam is introduced into a turbid medium, the transmitted light comprises three components, i.e., ballistic, snake, and diffuse photons.[10] The ballistic photons traverse the shortest path in the incident direction without scattering. The snake photons scatter slightly in the forward direction after traveling over relatively longer paths. The ballistic and snake components retain significant initial properties and information on the structures of the object submerged in the turbid medium. The diffuse photons travel long distances through multiple scattering within the medium and lose most of the image information. Thus the multiple-scattered diffuse light provides a noise background that deteriorates and, in extreme cases, may destroy any shadow image of structures inside the object. Therefore, the straightforward gated techniques are intuitive to image objects in scattering environment by detecting only the ballistic component but rejecting the diffuse component. The signal detected by these techniques is typically filtered by exploiting the spatial,[6,11] polarized,[7,12] and absorptive characteristic of the transmitted light.[8,13]

In some cases, the objects hidden in scattering environments are transparent such as the center of the liquid core in a fuel spray,[14,15] lymphatic system surrounded by normal tissue,[16] or adherent cells hidden by blood cells.[17] It is difficult to extract shape properties of these kinds of objects. For example, it is difficult to identify the structure features inside the liquid core using the straightforward gated or time-gated ballistic imaging techniques that are usually used to image high-contrast transverse features of the spray. The shape properties of the liquid core may be extracted by an ultrafast optical Kerr gate (OKG) with subpicosecond time-resolution, in which the ballistic photons with different optical path lengths can be selected by tuning the delay time of the switch beam. An OKG is obtained by inducing a temporary birefringence in a Kerr medium between two crossed polarizers.[18–20]

In the last two decades, femtosecond laser has been reported as a promising tool for laser processing,[21,22] ultrafast measurements and ultrafast imaging.[23] Using femtosecond laser, there are several time-gated methods to perform the time-gated optical imaging so far, such as time gate base on a b-barium borate crystal[24,25] and optical-parametric-amplification imaging.[26] Compared with these techniques, the OKG has no need of satisfaction of the phase-matching condition and can realize the switch time on the timescale of femtoseconds,[27,28] and it is satisfied with time-gated ballistic imaging.

In this Letter, we employ an OKG time-gated ballistic imaging system to image a transparent object in a turbid medium. The shape features of the object are manifested. In addition, combining the refractive index difference between the object and the surroundings, the thickness of the object is measured and the thickness distribution of the transparent object is mapped in the end.

To image the transparent object in the turbid environment, the shadowgraph arrangements depicted in Fig. 1 were experimentally used. Ultrafast laser pulses were generated by a Ti:sapphire laser system (Libra-USP-HE, Coherent Inc., USA), which can generate laser pulses with widths of less than 80 fs and energies of about 3.0 mJ per pulse at a repetition rate of 1 kHz, with a pulse spectrum centered at 800 nm. A schematic of OKG time-gated ballistic imaging system is shown in Fig. 1. The laser beam was split into two by using a beam splitter. The reflective part with 420 mW and the transmitted part with 180 mW

*Supported by the National Natural Science Foundation of China under Grant Nos 61427816 and 61690221, and the Collaborative Innovation Center of Suzhou Nano Science and Technology.

**Corresponding author. Email: jinhaisi@mail.xjtu.edu.cn

were used as the switch beam and the imaging beam, respectively. The switch beam was filtered using a short-pass filter. The polarization direction of the pump beam was rotated by 45° using a half-wave plate for maximizing gating efficiency. A stepper motor (MTS204, Boci, China) with 0.52 fs/step delay resolution was used to control the time delay between the imaging pulse and the switch pulse. The switch beam was focused on the optical Kerr medium with a size of 2 mm by lens L0. The carbon tetrachloride (CCl_4) filling a glass cuvette with a path length of 1 mm was used here as the optical Kerr material. The imaging beam was modulated by the transparent object that is formed with 1 mm width glass bands cut from a coverslip (refractive index, $n = 1.5$). To form the object, a layer of glass bands with 1 mm width distance was placed as a base, and another layer of glass bands with the same distribution was placed vertically onto the base ones. The thicknesses of the square-chessboard-shaped squares formed by the two layers of glass bands were 0 μm, 340 μm and 680 μm, which were measured by a micrometer with an error of about 10 μm. The modulated beam passed through a distilled water suspension of 15-μm-diameter polystyrene spheres with optical depth (OD) of approximately 3.6. The OD is defined as $-\ln(I/I_0)$, where I is the intensity of the ballistic light, and I_0 is the intensity of the incident light. An ultrafast optical Kerr gating method was used to directly determine the OD value.[29] The transmitted light was collected by the lens L1 (focal length, $f_1 = 150$ mm) placed at 150 mm from the object plane. The collected light was focused onto the cuvette after passing through the polarizer (P1) and the focus could overlap the focal point of the switch beam. The angle between the imaging beam and the switch beam was 12°. Thereafter, the light whose polarization was rotated passed through the analyzer (P2) was collected by the lens L2 ($f_2 = 250$ mm). The lens L2 was placed 250 mm behind the cuvette. The final OKG imaging beam was imaged onto a charge-coupled device camera (INFINITY3-1 M-NS-TPM, Lumenera Corporation, Ottawa, Canada). A long-pass filter (LPF) was placed before the camera to decrease the noise generated by the short-wave-band pump light scattering in the cuvette.

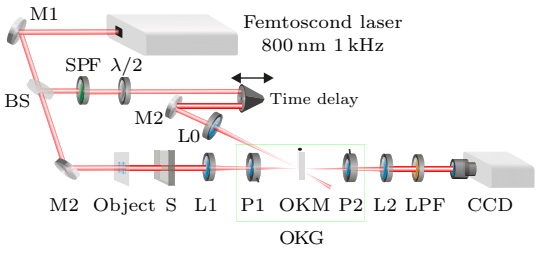

Fig. 1. OKG time-gated ballistic imaging setups. SPF: short-pass filter; $\lambda/2$: half-wave plate; BS: beam splitter; SPF: short-pass filter; LPF: long-pass filter; S: turbid medium; M1, M2 and M3: mirrors; L0, L1 and L2: lenses. The part marked with green box frame is the optical Kerr gate.

For comparison, a space-gated ballistic imaging arrangement was used. The laser beam was modulated by the object and passed through the suspensions in the above-mentioned experiments. The transmitted light was collected by the lens L1 placed at 150 mm from the object plane. An aperture (diameter, $d = 0.7$ mm) was placed in the focus plane to preferentially select the ballistic photons and quasi-ballistic photons based on their direction of propagation. Thereafter, the diverging beam was collected by the lens L2 and finally imaged onto the camera.

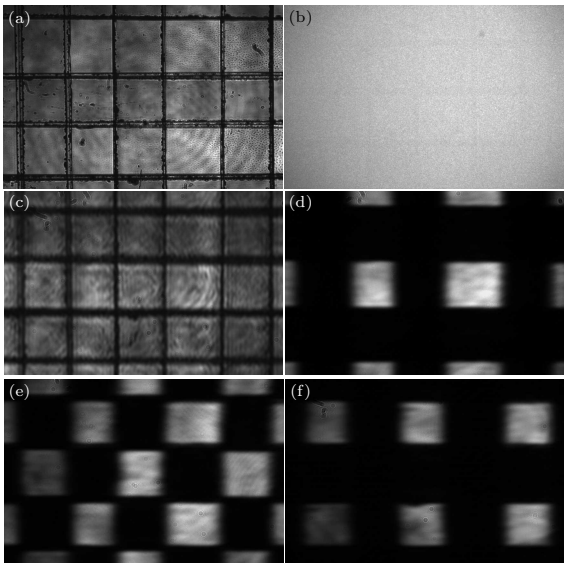

Fig. 2. Images of the object behind (a) water and (b) turbid medium. (c) Images of the object obtained using a spatial gated ballistic imaging arrangement behind the turbid medium. (d)–(f) Images obtained by tuning the time delay between switch pulse and imaging pulse at 0.40 ps, 0.96 ps and 1.52 ps, respectively.

Firstly, the image of the transparent object without turbid medium was directly imaged as reference. From Fig. 2(a), we can see that the edge feature of the object can be imaged but the transverse or the thickness features are unknown from the direct shadowgraph. Figure 2(b) shows the direct image of the object behind suspensions of 15-μm-diameter polystyrene spheres. The image is seriously disturbed by multiple scattered photons. Then, as shown in Fig. 2(c), the image of the object was obtained using the spatial gated ballistic imaging arrangement to compare with OKG time-gated ballistic images. We can see that the contrast of the latticed edge features is improved significantly by filtering multiple scattered photons. However, the thickness features of the transparent object behind the turbid medium also fail to be captured using this straightforward spatial gated technique.

Next, we employed the OKG time-gated ballistic imaging system to image the transparent object through the turbid medium. Figures 2(d)–2(f) show the images obtained by increasing the switch time delay between the switch pulse and the imaging pulse. The two-dimensional morphologies are different from the image obtained using the straightforward spatial gated technique. In detail, Fig. 2(c) shows the lat-

ticed features, while Figs. 2(d)–2(f) show the black and white checked patterns. In addition, the images of the object vary completely with the three different switch time delays. To explain this phenomenon, we further measured the time-resolved signal intensity of the OKG time-gated images by increasing the switch time delay. As shown in Fig. 3, there are three peaks marked by Roman numerals I, Ⅱ and Ⅲ and located at about 0.39 ps, 0.96 ps and 1.52 ps, which respectively correspond to Figs. 2(d)–2(f). The optical path length of the Kerr signal increases with the switch time delay, and the refractive index of the object used in our experiment is higher than that of the surrounding environment. Thus the signal peak at 0.40 ps in Fig. 3 corresponds to the ballistic photons passing by the transparent object. Based on the above discussion, the bright squares in Fig. 2(d) represent the background image and the black shadow depicts the transverse features of the transparent object. The signal peaks at 0.96 ps and 1.52 ps in Fig. 3 correspond to the ballistic photons that penetrate the transparent object with different optical path lengths. Thus the bright squares in Figs. 2(e) and 2(f) represent the areas with different thicknesses inside the object.

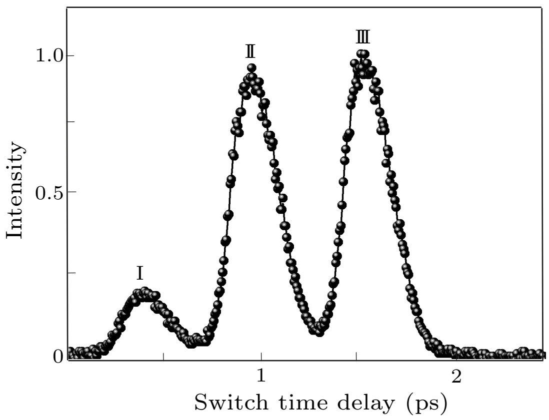

Fig. 3. Time-resolved signal intensity of the OKG time-gated images.

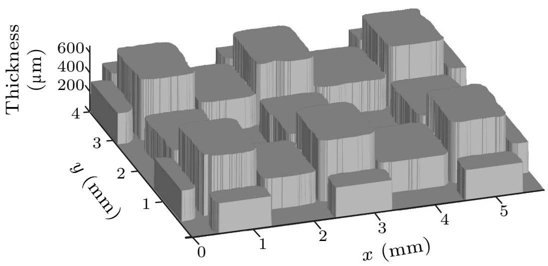

Fig. 4. Thickness distribution of the transparent object.

Furthermore, we quantitatively calculate the thickness L by $L = c\Delta t/\Delta n$, where $\Delta n = 0.5$ represents the refractive-index difference between the object and the surroundings, c is the velocity of light, and Δt is the intervals of the switch time delays between different signal peaks shown in Fig. 3. In terms of the time intervals 0.57 ps and 0.56 ps among the signal peaks I, Ⅱ and Ⅲ illustrated in Fig. 3, the thicknesses of the partial object shown in Figs. 2(e) and 2(f) are calculated to be approximately 342 μm and 672 μm. The maximum error was less than 3.6%. Then, we map the thickness distribution of the transparent object as shown in Fig. 4. To solve the nonuniformity of light field obtained with a Gaussian beam, the binarization processing is employed in this step.

In conclusion, we have employed an OKG time-gated ballistic imaging system to image a transparent object through a turbid medium. By tuning the switch time delay to detect the ballistic photons passing through the object and combining the path length with the refractive index, the thickness distribution of the object is measured. Moreover, we map the thickness distribution of the transparent object. The maximum error of the measured thickness is less than 3.6%.

References

[1] Bertolotti J, Putten E G, Blum C, Lagendijk A, Vos W L and Mosk A P 2012 *Nature* **491** 232
[2] Katz O, Small E, Guan Y and Silberberg Y 2014 *Optica* **1** 170
[3] Tong J Y, Tan W J, Si J H, Cheng F, Yi W H and Hou X 2012 *Chin. Phys. Lett.* **29** 024207
[4] Newman J A and Webb K J 2014 *Phys. Rev. Lett.* **113** 263903
[5] Soni N K, Vinu R V and Singh R K 2016 *Opt. Lett.* **41** 906
[6] Takahashi Y, Suzuki A, Furutaku S, Yamauchi K, Kohmura Y and Ishikawa T 2013 *Appl. Phys. Lett.* **102** 094102
[7] Guan J and Zhu J 2013 *Opt. Express* **21** 14152
[8] Tanzid M, Hogan N J, Sobhani A, Robatjazi H, Pediredla A K, Samaniego A, Veeraraghavan A and Halas N J 2016 *ACS Photon.* **3** 1787
[9] Zhou E H, Shibukawa A, Brake J, Ruan H and Yang C H 2016 *Optica* **3** 1107
[10] Wang L, Ho P P, Liu C, Zhang G and Alfano R R 1991 *Science* **253** 769
[11] Di B D, Zacharakis G and Leonetti M 2015 *Sci. Rep.* **5** 17406
[12] Vasefi F, MacKinnon N, Saager R B, Durkin A J, Chave R, Erik H L and Daniel L F 2015 *Sci. Rep.* **4** 4924
[13] Brezner B, Cahen S, Glasser Z, Sternklar S and Granot E 2015 *J. Biomed. Opt.* **20** 076006
[14] Wang Z, Ding H, Ma X, Xu H and Wyszynski M L 2016 *Appl. Energy* **163** 105
[15] Sbanski O, Roman V E, Kiefer W and Popp J 2000 *J. Opt. Soc. Am. A* **17** 313
[16] Munn L L and Padera T P 2014 *Microvasc. Res.* **96** 55
[17] AntonioáNetti P 2014 *Lab Chip* **14** 2499
[18] Ho P P and Alfano R R 1979 *Phys. Rev. A* **20** 2170
[19] Yu B L, Bykov A B, Qiu T, Ho P P, Alfano R R and Borrelli N 2003 *Opt. Commun.* **215** 407
[20] Duguay M A and Hansen J W 1969 *Appl. Phys. Lett.* **15** 192
[21] Chen T, Si J H, Hou X, Kanehira S and Miura K 2008 *Appl. Phys. Lett.* **93** 051112
[22] Si J H and Hirao K 2007 *Appl. Phys. Lett.* **91** 91105
[23] Ma Y C, Ren Y H, Si J H, Sun X H, Shi H T, Chen T, Chen F and Hou X 2012 *Appl. Surf. Sci.* **261** 722
[24] Dean J J, Lange C and Driel H M 2014 *Phys. Rev. B* **89** 024102
[25] Sajadi M, Quick M and Ernsting N P 2013 *Appl. Phys. Lett.* **103** 173514
[26] Pan X, Peng Y J, Wang J F, Lu X H, Ouyang X P, Chen J L, Jiang Y E, Fan W and Li X C 2013 *Chin. Phys. Lett.* **30** 014202
[27] Tan W J, Zhou Z G, Lin A, Si J H, Zhan P P and Wu B 2013 *Opt. Express* **21** 7740
[28] Zhan P P, Tan W J, Si J H, Xu S C, Tong J Y and Hou X 2014 *Appl. Phys. Lett.* **104** 211907
[29] Tong J Y, Yang Y, Si J H, Tan W J, Chen F, Yi W H and Hou X 2011 *Opt. Eng.* **50** 043607

Chinese Physics Letters

Volume 34 Number 10 October 2017